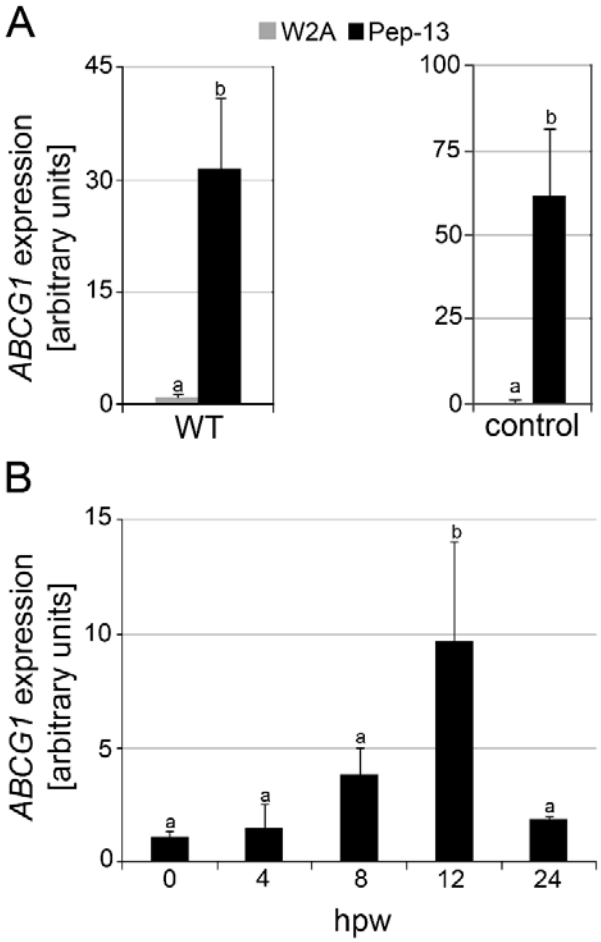

C

ATGTCAAGGATAGTAGCGGAAAATATGTTACAAGGGGGAGAAAATGTACA
ATTTTATGATCAAAGAGTACAACAAGCCATGGAGATGTCACAAGCCAGCG
CGTACTCTTCACCCACCCTAGGCCAAATGCTAAAGCGCGTGGGAGACGTG
AGAAAAGAAGTCACCGGCGACGAAACTCCGGTGCACCGGATTCTCGATAT
GAGTGATACTCAAAGCATATCATCTCACTCTCTTCCTTTTGTACTCTCCT
TCAACAACCTCACCTACAGCGTAAAAGTCCGCCGGAAAATGTCTTTTCCG
GCGATACTCCGGCAACCGGCCGCCGGAGTTTCCACCGGTGATCCCGTCGC
CGGAGAAAATCTGTTCACGAACACAAAATTCCTCCTGAACAATATCTCCG
GTGAGGCCCGGGACGGCGAGATAGTCGCCGTCCTGGGTGCATCAGGGTCG
GGGAAATCGACCCTGATCGATGCCCTCGCAAATAGGATCGCGAAGGAGAG
TTTAAAAGGAACGATAACGTTGAACGGAGAGCCACTCGATTCGAGATTGT
TGAAAGTAATCTCAGCATATGTAATGCAAGATGATCTTTTATATCCAATG
TTGACAGTTGAAGAAACGTTAATGTTTGCAGCTGAATTCAGATTGCCACG
TAGTTTATCAAAATCAAAAAAGAAAATGAGAGTTCAAGCTTTGATTGATC
AATTAGGACTACGAAATGCTGCAAAAACAATCATTGGTGATGAG*GTAACG*
TTATATATACAGTATAATTTTTTATCGATGCCTACAAACTGATCATATTT
*TTTTTTAACATTTAATAATAATTTACTATTTTGAACAACAG*GGTCATCGT
GGAGTGTCTGGTGGTGAAAGACGACGAGTTTCTATTGGAATTGATATTAT
TCATGACCCTATCATATTGTTTCTAGACGAACCAACCTCAGGTCTTGATT
CGACTAGTGCATACATGGTGGTGAAAGTTCTTCAACGAATTGCTCAAAGT
GGAAGTATTGTGATCATGTCAATTCATCAGCCAAGTTATCGAATTCTCGG
GTTATTGGATCGGATGCTCTTCTTGTCCCGTGGTCAAACGGTTTATAGCG
GGTCACCTATGAACCTCCCACATTTTTTTTCTGATTTTGGTCACCCAATT

CCGGATAGTGAAAATAGAACAGAGTTTGCTCTGGATCTGATTCGCGAACT
AGAAGGGTCCCCTGGAGGGACAAAAAGTTTGGTTGAGTTCAACAAAACAT
GGGAAAATACGAAAAGGAGTAATGAAAATCCTGAAATCCAAACACCTACT
CATGGATTGTCATTGAAAGAAGCGATTAGCGCGAGTATTTCAAGAGGGAA
GTTGGTTTCAGGGACAACGAGTGATATTCATACTAGTCCAGCATCAATGG
TTCCAACTTACGCGAATCCATTTTGGATTGAAATGCTTGTGTTGTCCAAG
AGATCATTTACGAATTCTTGGAGGGTGCCAGAGTTATTTGGTATCCGTCT
AGGGGCAATCGTGGTCACGGGGTTCATCCTAGCTACCATGTTTTGGCAAC
TTGATGATTCCCCTAAAGGGGTTCAAGAAAGGCTTGGTTTCTTTGCATTT
GCTATGTCAACAACTTTCTATACTTGCGCGGACGCGTTGCCTGTGTTCCT
CCAAGAGAGGTACATTTTCATGAGGGAGACAGCTTATAATGCTTATAGGA
GATCTTCCTATTGTCTATCTCATGCTATAGTTTCTTTGCCAGCATTGATC
TTTCTTAGCTTTGCATTTGCTGCTATAACTTTTTGGGCTGTAGGCCTTGT
AGGTGGATTTTCGGGCTTTTTGTTCTATTTCGCGATAATACTAGCCTCCT
TCTGGGCCGGGAATTCATTTGTCACGTTCCTCTCCGGTGTAGTTCCTAGT
GTCATGTTAGGTTACACCATAGTGGTCGCGATCCTAGCATATTTCCTCCT
CTTCTCAGGATTCTTCATCAATCGCGATAGGATTCCACCTTATTGGATAT
GGTTTCACTACCTATCTCTGGTGAAATATCCTTATGAAGCTGTGTTACAA
AATGAATTTGATGATGCAACAAAGTGTTTTGTCAAAGGGATTCAATTGTT
TGATAATTCACCACTTGGAAATGTGCCTAATGCATTGAAGGAAAAATTGT
TGAGTACAATGAGTAACACATTAAATGTCAAAATTACAAGTTCAACATGT
GTGACTACTGGGGCTGATATATTGGTTCAACAAGGGATTACTGATTTAAG
TAAGTGGAATTGTTTGTGGATTACTATTGCATGGGGGTTTTTCTTTAGGG
TTTTGTTTTACTTTAGCTTGTTGCTTGGAAGTAAGAACAAGAGAAGGTGA

D

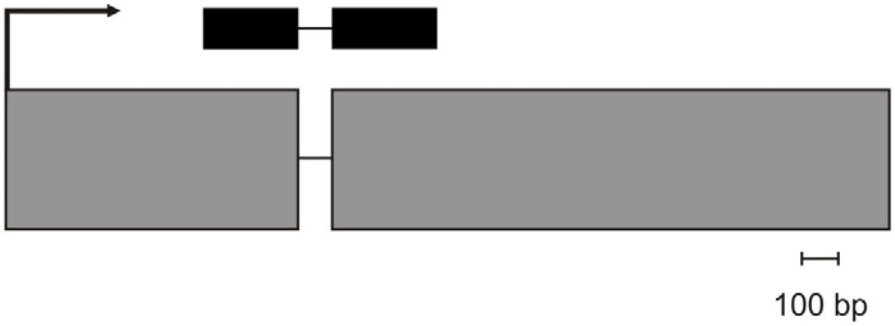

E

Supplemental Figure 1

Structure and expression of the *ABCG1* gene.

A: Pep-13-induced *ABCG1* expression. Left panel: POCI microarrays (Kloosterman et al., 2008) were hybridized with cDNA generated from RNA of potato leaves 8 hours after infiltration of 100 µM Pep-13 (black bar) or 100 µM W2A (grey bar). Data are derived from three independent experiments. Error bars represent SEM. Letters indicate statistically different values (t-test, $p \leq 0.03$).Right panel: Leaves of three week old wild type and transgenic plants carrying an empty vector (control) were infiltrated with 100 µM Pep-13 (black bar) or 100 µM W2A (grey bar). RNA was isolated 8 hours after treatment, reverse transcribed and analyzed for *ABCG1* transcript levels by qPCR. Expression of *EF1*α was used as a reference. Data are derived from two independent experiments (n=8). Error bars represent SEM. Letters indicate statistically different values (t-test, $p \leq 0.01$). B: Wound-induced expression of *ABCG1*. Leaves of wild type potato plants were wounded with a hemostat (hpw: hours post wounding). RNA was isolated from whole leaves at the time points indicated, reverse transcribed and analyzed for *ABCG1* transcript levels by qPCR. Expression of *EF1*α was used as a reference. Data are derived from two ($n \geq 4$) independent experiments. Error bars represent SD. Letters indicate significantly different values (one-way ANOVA, $p \leq 0.01$) C: Nucleotide sequence of the *ABCG1* gene. The sequence was obtained from the genome sequence of *Solanum tuberosum* group *phureja* (Xu et al., 2011; XM_006345853.1, http://www.ncbi.nlm.nih.gov/). Intron sequences are shown in italics. D: Schematic structure of the *ABCG1* gene and position of the *ABCG1*-RNAi construct. E: Schematic structure of the ABCG1 protein. The ATP binding domain (grey) and the six predicted transmembrane domains (black) are shown.

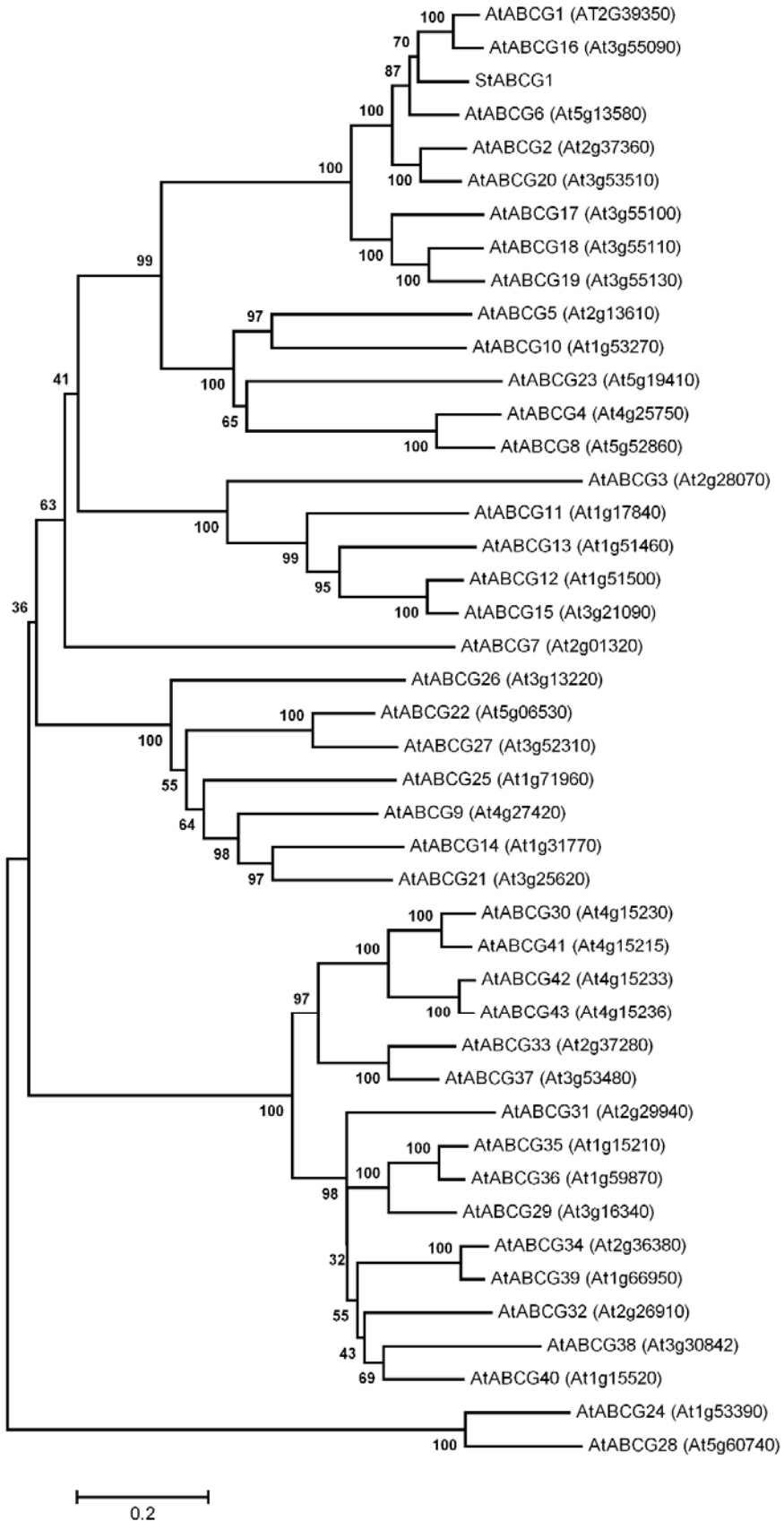
AtABCG1 (AT2G39350)
AtABCG16 (At3g55090)
StABCG1
AtABCG6 (At5g13580)
AtABCG2 (At2g37360)
AtABCG20 (At3g53510)
AtABCG17 (At3g55100)
AtABCG18 (At3g55110)
AtABCG19 (At3g55130)
AtABCG5 (At2g13610)
AtABCG10 (At1g53270)
AtABCG23 (At5g19410)
AtABCG4 (At4g25750)
AtABCG8 (At5g52860)
AtABCG3 (At2g28070)
AtABCG11 (At1g17840)
AtABCG13 (At1g51460)
AtABCG12 (At1g51500)
AtABCG15 (At3g21090)
AtABCG7 (At2g01320)
AtABCG26 (At3g13220)
AtABCG22 (At5g06530)
AtABCG27 (At3g52310)
AtABCG25 (At1g71960)
AtABCG9 (At4g27420)
AtABCG14 (At1g31770)
AtABCG21 (At3g25620)
AtABCG30 (At4g15230)
AtABCG41 (At4g15215)
AtABCG42 (At4g15233)
AtABCG43 (At4g15236)
AtABCG33 (At2g37280)
AtABCG37 (At3g53480)
AtABCG31 (At2g29940)
AtABCG35 (At1g15210)
AtABCG36 (At1g59870)
AtABCG29 (At3g16340)
AtABCG34 (At2g36380)
AtABCG39 (At1g66950)
AtABCG32 (At2g26910)
AtABCG38 (At3g30842)
AtABCG40 (At1g15520)
AtABCG24 (At1g53390)
AtABCG28 (At5g60740)
0.2

Supplemental Figure 2

Evolutionary relationships of St-ABCG1 and At-ABCG1 to 43. The amino acid sequences of St-ABCG1 and At-ABCG1 to At-ABCG43 were compared. The evolutionary history was inferred using the Neighbor-Joining method (Saitou and Nei, 1987). The optimal tree with the sum of branch length = 11.04991171 is shown. The percentage of replicate trees in which the associated taxa clustered together in the bootstrap test (1000 replicates) are shown next to the branches (Felsenstein, 1985). The tree is drawn to scale, with branch lengths in the same units as those of the evolutionary distances used to infer the phylogenetic tree. The evolutionary distances were computed using the Poisson correction method (Zuckerkandl and Pauling, 1965) and are in the units of the number of amino acid substitutions per site. All positions containing gaps and missing data were eliminated from the dataset (complete deletion option). There were a total of 453 positions in the final dataset. Phylogenetic analyses were conducted in MEGA4 (Tamura et al., 2007).

A

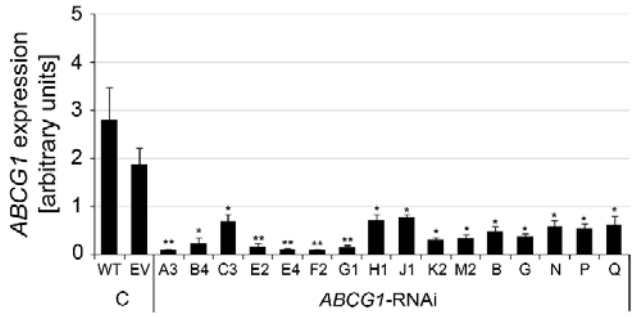

B

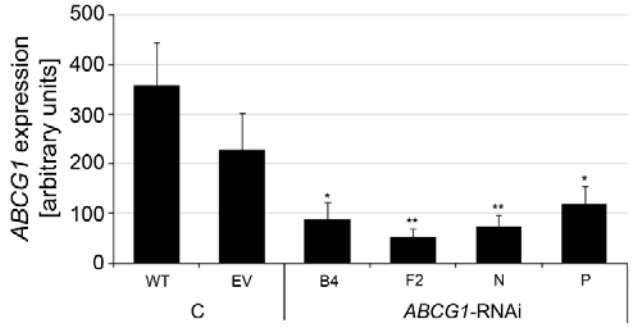

Supplemental Figure 3

Reduced *ABCG1* expression in *ABCG1*-RNAi lines.

A: *ABCG1* expression in wounded *ABCG1*-RNAi plants. RNA was isolated from potato leaves six hours post wounding, reverse transcribed and analyzed for *ABCG1* transcript levels by qPCR. Data are derived from three independent experiments (wild type: n=12; empty vector plants: n=12; *ABCG1*-RNAi plants: n=6). Error bars represent SEM. Significance analysis of differences between *ABCG1*-RNAi and control was performed by t-test (* $p<0.05$, ** $p<0.01$). B: *ABCG1* expression in *ABCG1*-RNAi tuber skin. RNA was isolated from tuber skin of three-month-old potato plants grown in a greenhouse. RNA was reverse transcribed and analyzed for *ABCG1* expression by qPCR. Data are derived from two independent experiments (n=4). Error bars represent SEM. Significance analysis of differences between *ABCG1*-RNAi, EV and WT was performed by t-test (two-tailed, unequal variances): *$p\leq0.05$; **$p\leq0.01$.

A

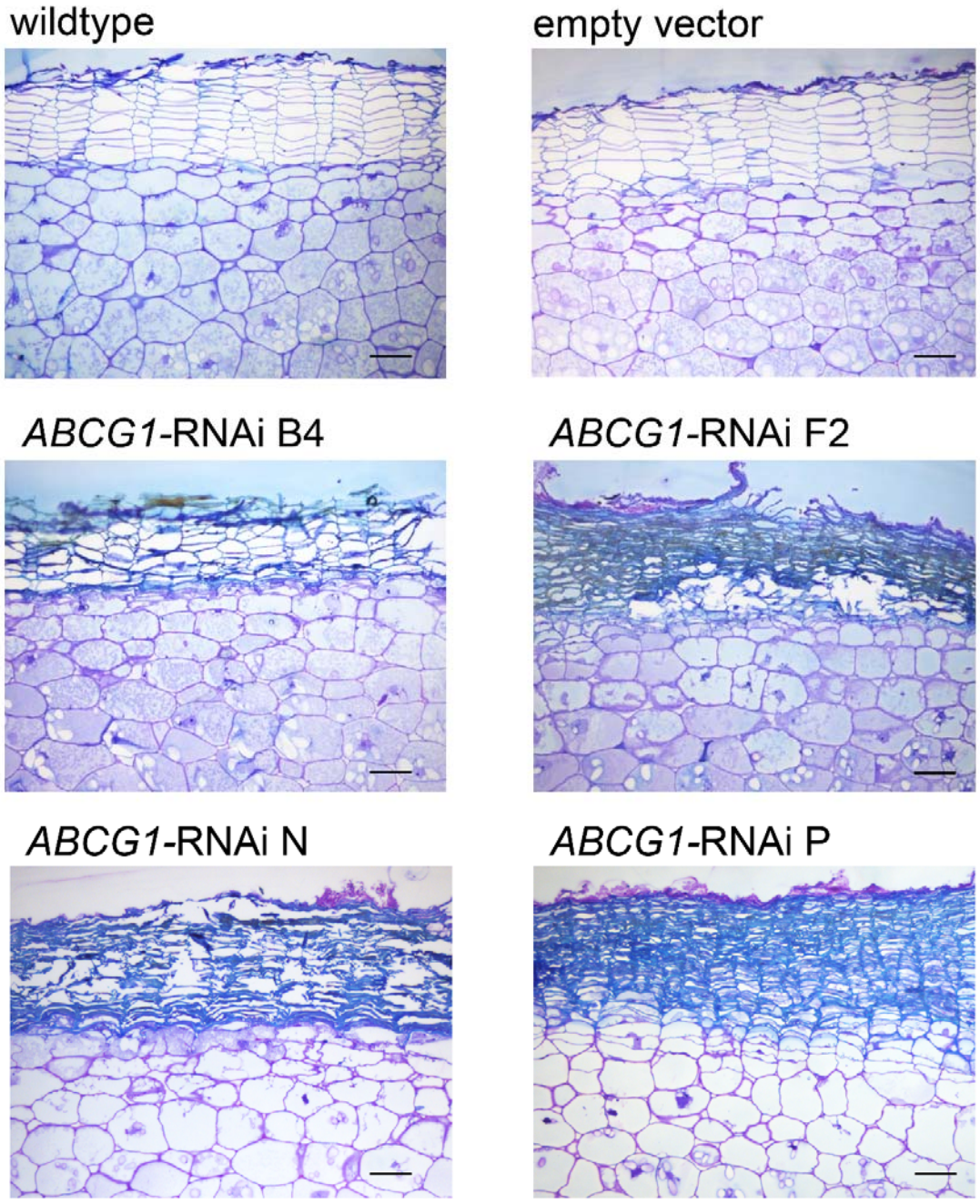
wildtype
empty vector
ABCG1-RNAi B4
ABCG1-RNAi F2
ABCG1-RNAi N
ABCG1-RNAi P

B

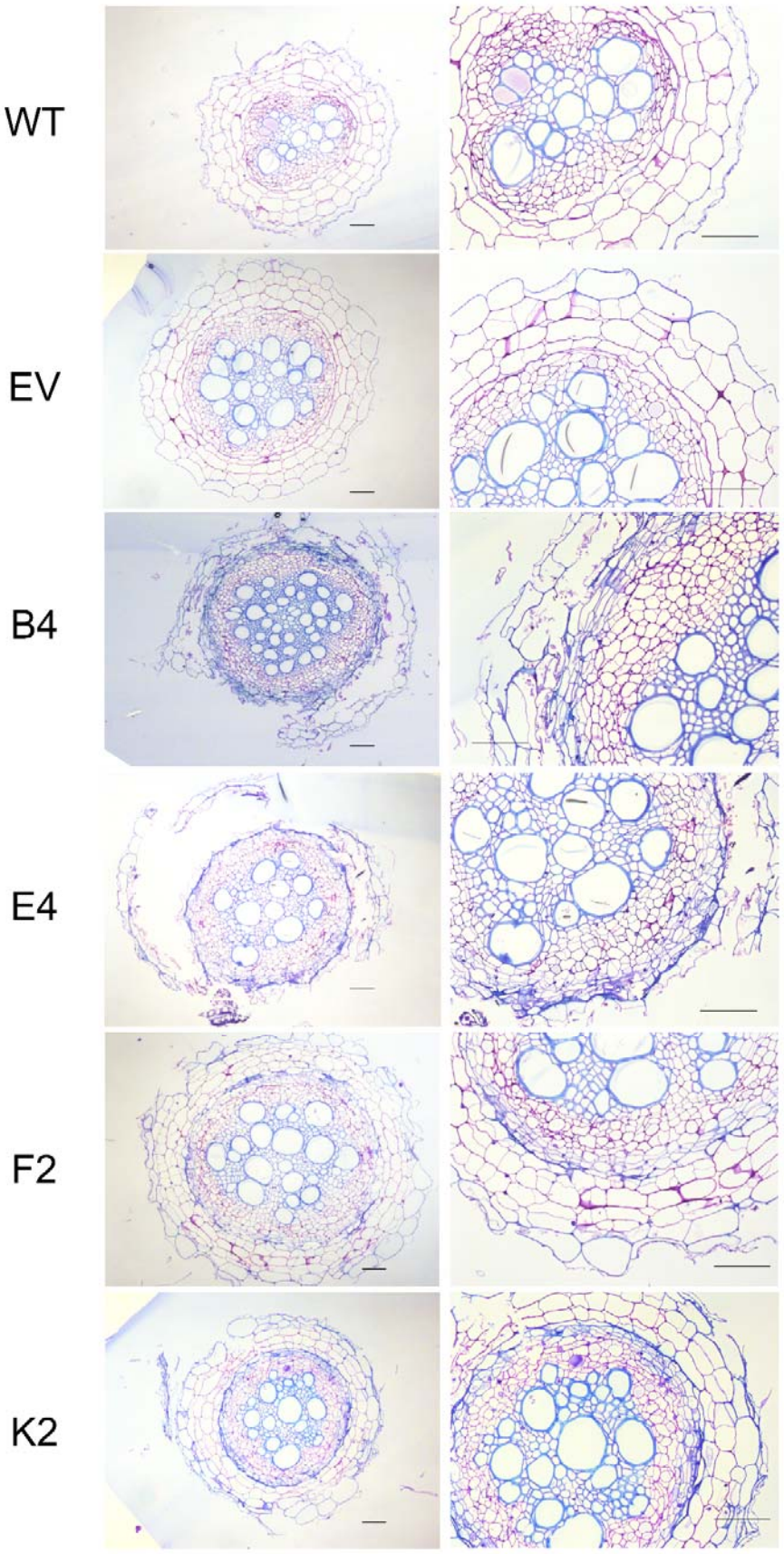

Supplemental Figure 4

Morphological alterations in tuber periderm and roots of *ABCG1*-RNAi lines. A: Microscopy of toluidine blue-stained periderm cross sections of wild type, empty vector and four independent *ABCG1*-RNAi plants. Tubers were harvested from three months old, greenhouse grown potato plants and analyzed after one week of storage at 4°C. Scale bars represent 5 µm. B: Microscopy of toluidine blue-stained root cross sections of wild type, empty vector and *ABCG1*-RNAi plants. Roots were harvested from three-month-old, greenhouse grown potato plants. Scale bars represent 1 µm.

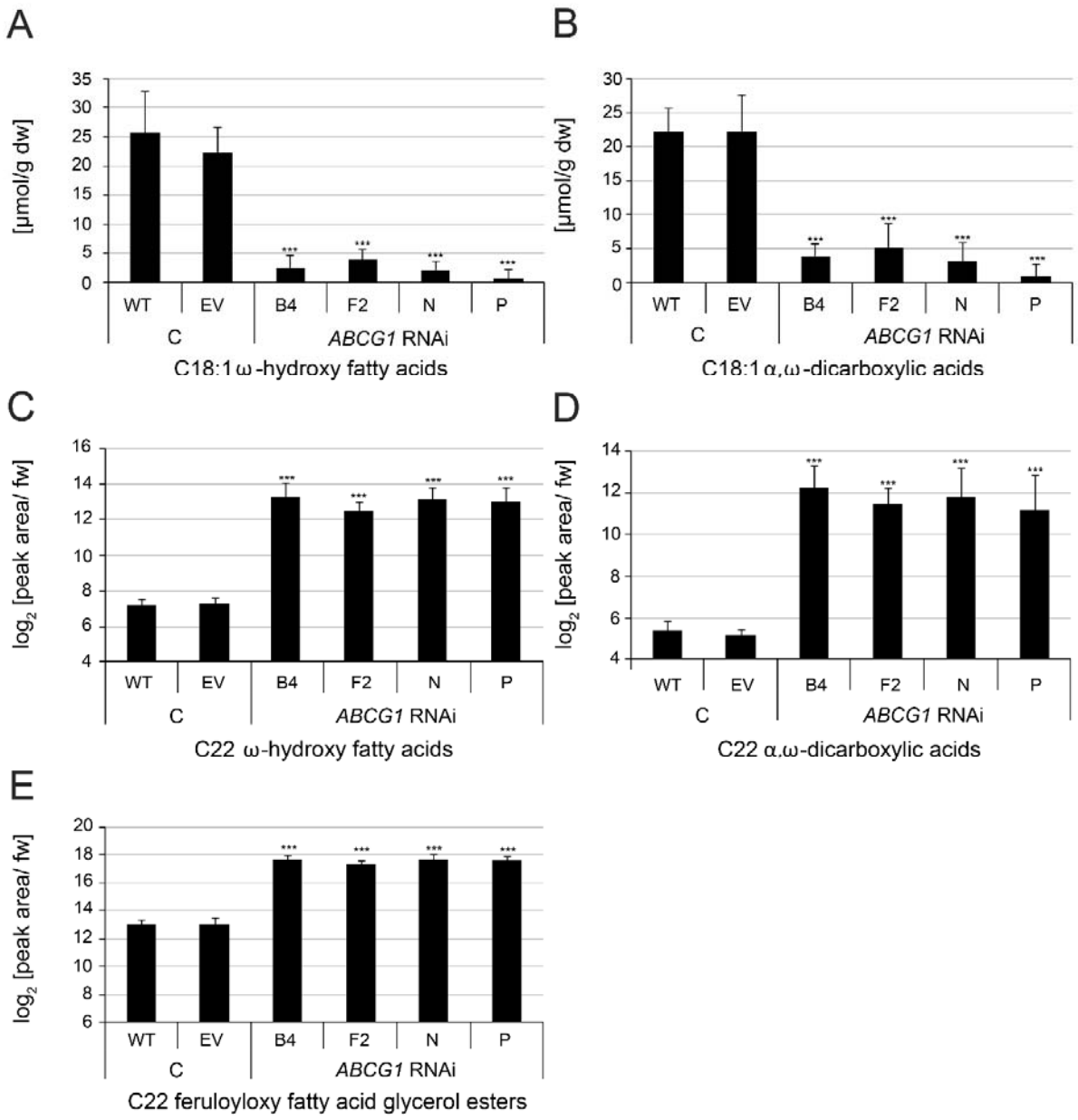

Supplemental Figure 5

Suberin composition in individual *ABCG1*-RNAi lines. A: Relative Quantification of C18:1 ω-hydroxy fatty acid as well as α,ω-DCA (B) of wild type, empty vector and *ABCG1*-RNAi tuber periderm.

Digested and delipidated periderm disks were depolymerized and analyzed by GC/MS. Resulting peak areas were normalized to the peak area of the corresponding internal standard and to dry weight. Values shown represent medians ± SD. Data are derived from

two independent experiments (n=8). Statistical analysis was performed by *t*-test (two-tailed, unequal variances): ***$p \leq 0.001$.

C: Relative quantification of C22 ω-hydroxy fatty acids, C22 α,ω-dicarboxylic acids (D) and C22 feruloyloxy fatty acid glycerol esters (E) in apolar extracts of wild type, empty vector and *ABCG1*-RNAi periderm. Methyl *tert*-butyl ether extracts of tuber periderm were prepared and analyzed by UPLC/PDA/ESI(-)-QTOFMS. Resulting peak areas were normalized to fresh weight and $\log_2$-transformed. Values shown represent medians ± SD. Data are derived from two independent experiments (n=8). Statistical analysis was performed by *t*-test (two-tailed, unequal variances): ***$p \leq 0.001$.

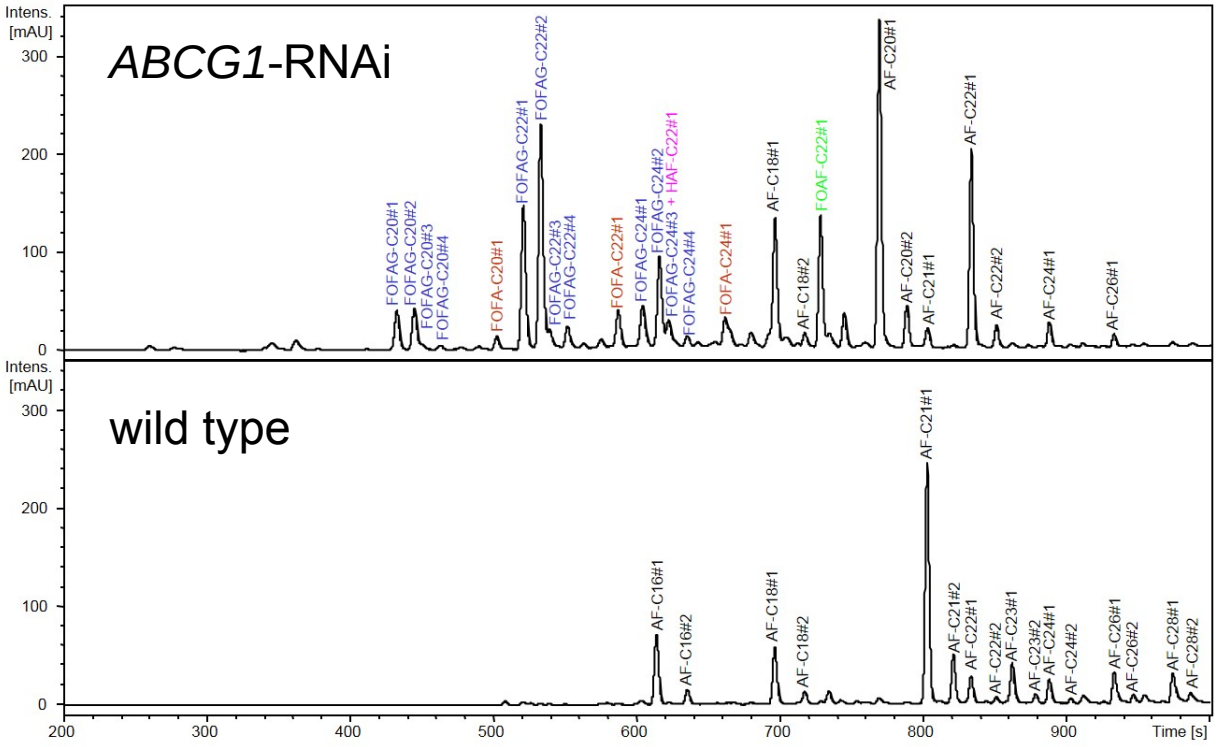

Supplemental Figure 6

UV chromatograms (324 nm) obtained from apolar extracts of *ABCG1*-RNAi and wild type tuber periderm. Major ferulic acid conjugates are labeled as follows: AF, Alkyl Ferulate; HAF, HydroxyAlkyl Ferulate; FOAF, FeruloyloxyAlkyl Ferulate; FOFA, FeruloylOxyFatty Acid; FOFAG, FeruloylOxyFatty Acid Glycerol ester.

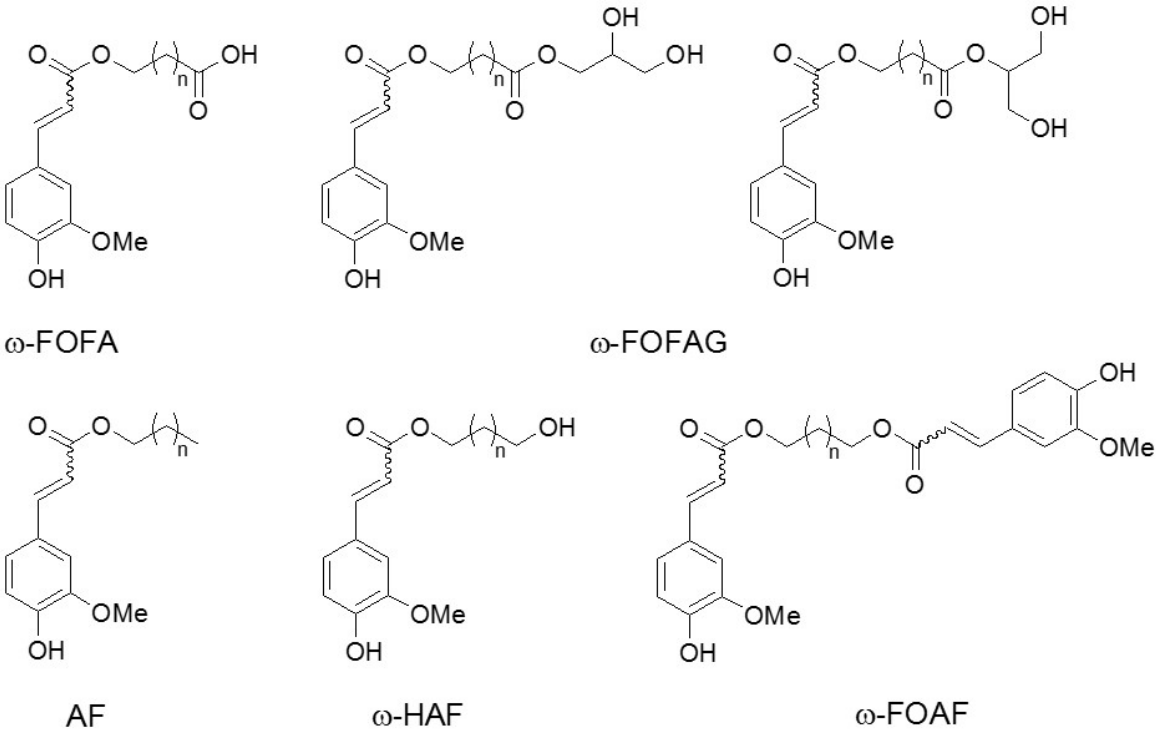

Supplemental Figure 7

Putative molecular structures of ferulic acid conjugates detectable in apolar extracts of *ABCG1*-RNAi tuber periderm. ω-FOFA, ω-feruloyloxy fatty acid; ω-FOFAG, ω-feruloyloxy fatty acid glycerol ester; AF, alkyl ferulate; ω-HAF, ω-hydroxy alkyl ferulate; ω-FOAF, ω-feruloyloxy alkyl ferulate.

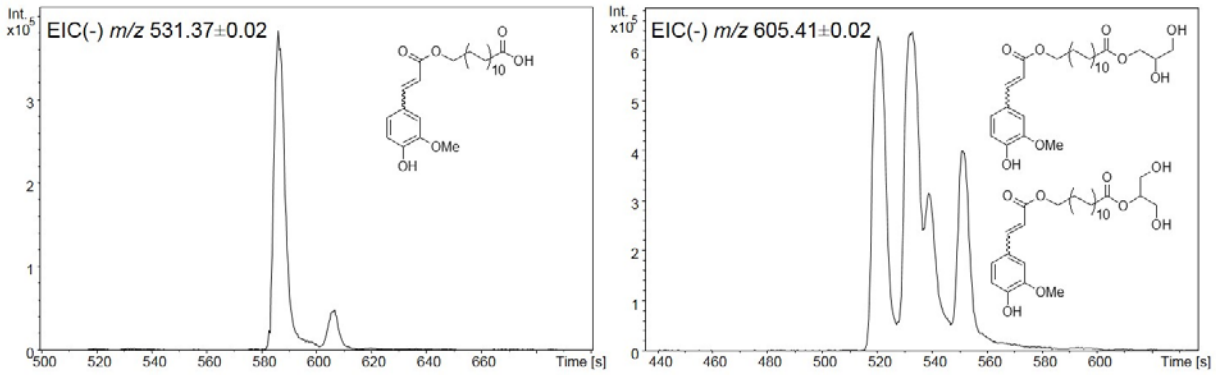

Supplemental Figure 8

Extracted ion chromatograms (EICs) corresponding to deprotonated molecular ions of feruloyloxy docosanoic acid (left) and feruloyloxy docosanoyl glycerol (right) obtained from apolar extracts of *ABCG1*-RNAi tuber periderm by UPLC/PDA/ESI(-)-QTOFMS.

Under the applied chromatographic conditions, two isomeric forms were separable for alkyl ferulates, hydroxy alkyl ferulates, feruloyloxy alkyl ferulates and feruloyloxy fatty acids due to the occurrence of (*E*)- and (*Z*)-configured feruloyl moieties. For feruloyloxy fatty acid glycerol esters, twice the number of isomers could be resolved due to the presence of (*E*)- and (*Z*)-configured feruloyl as well as 1-/3- and 2-acylated glycerol moieties.

Supplemental Table 1. Analytical Data of 1-Trimethylsilyloxy Alkanes Detected by GC/EI-QMS.

analyte	elemental comp.	M	ret. time *[min]*	quantifier ion *m/z* (rel. int.[%])	qualifier ions *m/z* (rel. int.[%])		MF[1]	internal standard for quantification
C15:0	$C_{18}H_{40}OSi$	300	10.78	285 (100)	103 (17)	75 (49)	885	internal standard
C16:0	$C_{19}H_{42}OSi$	314	11.87	299 (100)	103 (25)	-	-[2]	pentadecanol (1TMS)
C18:0	$C_{21}H_{46}OSi$	342	13.94	327 (100)	103 (19)	75 (51)	925	pentadecanol (1TMS)
C20:0	$C_{23}H_{50}OSi$	370	15.89	355 (100)	103 (21)	75 (60)	899	pentadecanol (1TMS)
C22:0	$C_{25}H_{54}OSi$	398	17.73	383 (100)	103 (18)	75 (40)	910	pentadecanol (1TMS)
C24:0	$C_{27}H_{58}OSi$	426	19.37	411 (100)	103 (22)	75 (48)	910	pentadecanol (1TMS)
C26:0	$C_{29}H_{62}OSi$	454	20.89	439 (100)	103 (19)	75 (40)	942	pentadecanol (1TMS)
C28:0	$C_{31}H_{66}OSi$	482	22.35	467 (100)	103 (14)	75 (22)	918	pentadecanol (1TMS)
C30:0	$C_{33}H_{70}OSi$	510	23.64	495 (100)	103 (17)	-	692[3]	pentadecanol (1TMS)

[1] match factor obtained from NIST MS Search 2.0 using NIST/EPA/NIH Mass Spectral Library 2011
[2] co-eluting with the major isomer of methyl ferulate (1TMS)
[3] co-eluting with methyl tricontanoate

Supplemental Table 2. Analytical Data of α,ω-Dicarboxylic Acid Dimethyl Esters Detected by GC/EI-QMS.

analyte	elemental comp.	M	ret. time *[min]*	quantifier ion *m/z* (rel. int.[%])	qualifier ions *m/z* (rel. int.[%])		MF[1]	internal standard for quantification
C16:0	$C_{18}H_{34}O_4$	314	14.94	98 (87)	283 (16)	74 (100)	823	methyl heptadecanoate
C18:1Δ9	$C_{20}H_{36}O_4$	340	16.64	276 (43)	309 (21)	340 (3)	-[2,3]	methyl heptadecanoate
C20:0	$C_{22}H_{42}O_4$	370	18.64	98 (64)	339 (17)	74 (100)	805	methyl heptadecanoate
C22:0	$C_{24}H_{46}O_4$	398	20.25	98 (64)	367 (13)	74 (100)	882	methyl heptadecanoate
C24:0	$C_{26}H_{50}O_4$	426	21.77	98 (59)	395 (12)	74 (100)	-[2]	methyl heptadecanoate

[1] match factor obtained from NIST MS Search 2.0 using NIST/EPA/NIH Mass Spectral Library 2011
[2] spectrum not contained in NIST/EPA/NIH Mass Spectral Library 2011
[3] for a reference spectrum see Kolattukudy and Agrawal, *Lipids* (1974) **9**, 682-691

Supplemental Table 3. Analytical Data of Fatty Acid Methyl Esters Detected by GC/EI-QMS.

analyte	elemental comp.	M	ret. time *[min]*	quantifier ion *m/z* (rel. int.[%])	qualifier ions *m/z* (rel. int.[%])		MF[1]	internal standard for quantification
C17:0	$C_{18}H_{36}O_2$	284	12.56	74 (100)	87 (68)	284 (8)	908	internal standard
C20:0	$C_{21}H_{42}O_2$	326	15.64	74 (100)	87 (71)	326 (13)	798	methyl heptadecanoate
C22:0	$C_{23}H_{46}O_2$	354	17.54	74 (100)	87 (72)	354 (18)	872	methyl heptadecanoate
C24:0	$C_{25}H_{50}O_2$	382	19.23	74 (100)	87 (74)	382 (20)	852	methyl heptadecanoate
C26:0	$C_{27}H_{54}O_2$	410	20.80	74 (100)	87 (73)	410 (25)	898	methyl heptadecanoate
C28:0	$C_{29}H_{58}O_2$	438	22.28	74 (100)	87 (79)	438 (40)	880	methyl heptadecanoate
C30:0	$C_{31}H_{62}O_2$	466	23.62	74 (100)	87 (82)	466 (40)	856	methyl heptadecanoate

[1] match factor obtained from NIST MS Search 2.0 using NIST/EPA/NIH Mass Spectral Library 2011

Supplemental Table 4. Analytical Data of ω-Trimethylsilyloxy Fatty Acid Methyl Esters Detected by GC/EI-QMS.

analyte	elemental comp.	M	ret. time *[min]*	quantifier ion *m/z* (rel. int.[%])	qualifier ions *m/z* (rel. int.[%])		MF[1]	internal standard for quantification
C15:0	$C_{19}H_{40}O_3Si$	344	14.23	297 (100)	329 (43)	146 (9)	-[2]	internal standard
C16:0	$C_{20}H_{42}O_3Si$	358	15.22	311 (100)	343 (26)	146 (10)	860	methyl 15-hydroxy pentadecanoate (1TMS)
C18:0	$C_{22}H_{46}O_3Si$	386	17.14	339 (100)	371 (32)	146 (13)	-[2]	methyl 15-hydroxy pentadecanoate (1TMS)
C18:1Δ9	$C_{22}H_{44}O_3Si$	384	16.94	337 (52)	369 (94)	146 (14)	824[3]	methyl 15-hydroxy pentadecanoate (1TMS)
C20:0	$C_{24}H_{50}O_3Si$	414	18.80	367 (100)	399 (55)	146 (18)	-[2]	methyl 15-hydroxy pentadecanoate (1TMS)
C22:0	$C_{26}H_{54}O_3Si$	442	20.39	395 (100)	427 (44)	146 (24)	801	methyl 15-hydroxy pentadecanoate (1TMS)
C24:0	$C_{28}H_{58}O_3Si$	470	21.86	423 (100)	455 (53)	146 (24)	-[2]	methyl 15-hydroxy pentadecanoate (1TMS)
C26:0	$C_{30}H_{62}O_3Si$	498	23.24	451 (100)	483 (63)	146 (29)	-[2]	methyl 15-hydroxy pentadecanoate (1TMS)
C28:0	$C_{32}H_{66}O_3Si$	526	24.53	479 (100)	511 (80)	146 (36)	-[2]	methyl 15-hydroxy pentadecanoate (1TMS)
C30:0	$C_{34}H_{70}O_3Si$	554	25.74	507 (100)	539 (77)	146 (25)	-[2]	methyl 15-hydroxy pentadecanoate (1TMS)

[1] match factor obtained from NIST MS Search 2.0 using NIST/EPA/NIH Mass Spectral Library 2011
[2] spectrum not contained in NIST/EPA/NIH Mass Spectral Library 2011
[3] for a reference spectrum see Brieskorn and Binnemann, *Z. Lebensm. Unters. Forsch.* (1974) **154**, 213-220

Supplemental Table 5. Analytical Data of Feruloyloxy Fatty Acids Detected by UPLC/ESI(-)-QTOFMS.

analyte	elemental comp.	ret. time [s]	quantifier ion				prominent fragment ions upon CID precursor ion@collision energy: *m/z* (rel. int. [%], ion type[3])
			type	measured *m/z*	error *ppm*	mSigma[1]	
C16:0	$C_{26}H_{40}O_6$	316[2]	$[M-H]^-$	447.2753	0.2	19	**447@30 eV:** 447 (29), 415 (37, **a**), 345 (27, **b**), 271 (64, **c**), 193 (14), 175 (100), 160 (31)
C18:0	$C_{28}H_{44}O_6$	410[2]	$[M-H]^-$	475.3056	1.9	9.7	**475@30 eV:** 475 (49), 443 (32, **a**), 373 (25, **b**), 299 (62, **c**), 193 (13), 175 (100), 160 (25)
C18:1	$C_{28}H_{42}O_6$	347[2]	$[M-H]^-$	473.2895	2.9	6.4	**473@30 eV:** 473 (30), 441 (27, **a**), 371 (3, **b**), 297 (56, **c**), 193 (13), 175 (100), 160 (23)
C18:2	$C_{28}H_{40}O_6$	288[2]	$[M-H]^-$	471.2757	1.0	16	**471@30 eV:** 471 (28), 439 (26, **a**), 369 (8, **b**), 295 (79, **c**), 193 (23), 175 (100), 160 (30)
C19:0	$C_{29}H_{46}O_6$	456[2]	$[M-H]^-$	489.3205	3.4	28	**489@30 eV:** 489 (60), 457 (33, **a**), 387 (20, **b**), 313 (51, **c**), 193 (18), 175 (100), 160 (18)
C20:0	$C_{30}H_{48}O_6$	501[2]	$[M-H]^-$	503.3372	1.2	9.2	**503@30 eV:** 503 (56), 471 (23, **a**), 401 (13, **b**), 327 (48, **c**), 193 (12), 175 (100), 160 (14)
C21:0	$C_{31}H_{50}O_6$	544[2]	$[M-H]^-$	517.3527	1.5	6.4	**517@30 eV:** 517 (61), 485 (18, **a**), 415 (10, **b**), 341 (40, **c**), 193 (12), 175 (100), 160 (11)
C22:0	$C_{32}H_{52}O_6$	585[2]	$[M-H]^-$	531.3707	3.0	9.7	**531@30 eV:** 531 (68), 499 (18, **a**), 429 (9, **b**), 355 (37, **c**), 193 (12), 175 (100), 160 (12)
C23:0	$C_{33}H_{54}O_6$	625[2]	$[M-H]^-$	545.3832	2.9	13	**545@30 eV:** 545 (83), 513 (16, **a**), 443 (5, **b**), 369 (35, **c**), 193 (14), 175 (100), 160 (9)
C24:0	$C_{34}H_{56}O_6$	663[2]	$[M-H]^-$	559.3992	2.2	5.1	**559@30 eV:** 559 (76), 527 (12, **a**), 457 (5, **b**), 383 (32, **c**), 193 (11), 175 (100), 160 (8)
C25:0	$C_{35}H_{58}O_6$	700[2]	$[M-H]^-$	573.4138	3.9	9.4	**573@30 eV:** 573 (90), 541 (5, **a**), 471 (4, **b**), 397 (21, **c**), 193 (10), 175 (100), 160 (7)
C26:0	$C_{36}H_{60}O_6$	735[2]	$[M-H]^-$	587.4313	0.7	18	**587@30 eV:** 587 (100), 555 (8, **a**), 485 (3, **b**), 411 (26, **c**), 193 (14), 175 (91), 160 (6)
C28:0	$C_{38}H_{64}O_6$	796[2]	$[M-H]^-$	615.4612	2.9	21	**615@30 eV:** 615 (100), 583 (7, **a**), 513 (2, **b**), 439 (22, **c**), 193 (8), 175 (95), 160 (7)

[1] goodness of fit between measured and calculated isotope pattern (Bruker Daltonics, Data Analysis 4.0)
[2] major (*E*)-isomer, minor (*Z*)-isomer elutes 16 s later, isomer ratio (E)/(Z) ≈ 10:1
[3] elemental composition of fragment ions supported by accurate mass measurements (± 15 ppm), **a**=$[M-H-CH_4O]^-$, **b**=$[M-H-C_5H_{10}O_2]^-$, **c**=$[M-H-C_{10}H_8O_3]^-$, *m/z* 193=$[C_{10}H_9O_4]^-$ Ferulate, *m/z* 175=$[C_{10}H_7O_3]^-$, *m/z* 160=$[C_9H_4O_3]^{\bullet-}$

Supplemental Table 6. Analytical Data of Feruloyloxy Fatty Acid Glycerol Esters Detected by UPLC/ESI(-)-QTOFMS.

analyte	elemental comp.	ret. time [s]	quantifier ion				prominent fragment ions upon CID
			type	measured *m/z*	error *ppm*	mSigma[1]	precursor ion@collision energy: *m/z* (rel. int. [%], ion type[3])
C16:0	$C_{29}H_{46}O_8$	246/257[2]	$[M-H]^-$	521.3106	2.7	11	**521@30 eV:** 521 (11), 506 (20, **a**), 447 (100, **b**), 429 (52, **c**), 271 (18, **d**), 193(3), 175 (65)
C18:0	$C_{31}H_{50}O_8$	339/350[2]	$[M-H]^-$	549.3433	0.0	4.2	**549@30 eV:** 549 (32), 534 (17, **a**), 475 (100, **b**), 457 (69, **c**), 299 (17, **d**), 193(7), 175 (65)
C18:1	$C_{31}H_{48}O_8$	280/290[2]	$[M-H]^-$	547.3277	0.1	4.2	**547@30 eV:** 547 (14), 532 (22, **a**), 473 (100, **b**), 455 (71, **c**), 297 (25, **d**), 193(9), 175 (89)
C18:2	$C_{31}H_{46}O_8$	225/233[2]	$[M-H]^-$	545.3119	0.2	11	**545@30 eV:** 545 (15), 530 (19, **a**), 471 (85, **b**), 453 (71, **c**), 295 (29, **d**), 193(11), 175 (100)
C19:0	$C_{32}H_{52}O_8$	385/397[2]	$[M-H]^-$	563.3576	2.4	21	**563@30 eV:** 563 (29), 548 (13, **a**), 489 (100, **b**), 471 (79, **c**) 193(5), 175 (50)
C20:0	$C_{33}H_{54}O_8$	431/443[2]	$[M-H]^-$	577.3750	0.7	6.3	**577@30 eV:** 577 (32), 562 (17, **a**), 503 (100, **b**), 485 (62, **c**), 327 (11, **d**), 193(6), 175 (57)
C21:0	$C_{34}H_{56}O_8$	476/488[2]	$[M-H]^-$	591.3894	1.4	1.9	**591@30 eV:** 591 (38), 576 (15, **a**), 517 (100, **b**), 499 (56, **c**), 341 (10, **d**), 193(5), 175 (49)
C22:0	$C_{35}H_{58}O_8$	519/531[2]	$[M-H]^-$	605.4058	0.2	2.0	**605@30 eV:** 605 (43), 590 (12, **a**), 531 (100, **b**), 513 (51, **c**), 355 (8, **d**), 193(5), 175 (46)
C23:0	$C_{36}H_{60}O_8$	561/573[2]	$[M-H]^-$	619.4206	1.5	4.1	**619@30 eV:** 619 (60), 604 (11, **a**), 545 (100, **b**), 527 (52, **c**), 369 (8, **d**), 193(5), 175 (43)
C24:0	$C_{37}H_{62}O_8$	601/614[2]	$[M-H]^-$ **c**	633.4355	2.7	4.4	**633@30 eV:** 633 (67), 618 (10, **a**), 559 (100, **b**), 541 (49, **c**), 383 (8, **d**), 193(4), 175 (39)
C25:0	$C_{38}H_{64}O_8$	641/653[2]	$[M-H]^-$ **c**	647.4517	1.8	8.0	**647@30 eV:** 647 (81), 632 (10, **a**), 573 (100, **b**), 555 (47, **c**), 397 (8, **d**), 193(5), 175 (39)
C26:0	$C_{39}H_{66}O_8$	679/690[2]	$[M-H]^-$ **c**	661.4672	2.0	3.0	**661@30 eV:** 661 (100), 646 (9, **a**), 587 (98, **b**), 569 (47, **c**), 411 (6, **d**), 193(4), 175 (37)
C28:0	$C_{41}H_{70}O_8$	747/759[2]	$[M-H]^-$ **c**	689.4998	0.0	36	**689@30 eV:** 689 (100), 674 (7, **a**), 615 (83, **b**), 597 (19, **c**), 193(4), 175 (51)

[1] goodness of fit between measured and calculated isotope pattern (Bruker Daltonics, Data Analysis 4.0)
[2] probably constitutional isomers with different linkage between the fatty acid and glycerol, isomer ratio in the range from 3:1 to 1:1
[3] elemental composition of fragment ions supported by accurate mass measurements (± 15 ppm), **a**=$[M-H-CH_3]^{\bullet-}$, **b**=$[M-H-C_3H_6O_2]^-$,**c**=$[M-H-C_3H_8O_3]^-$, **d**=$[M-H-C_3H_6O_2-C_{10}H_8O_3]^-$, *m/z* 193=$[C_{10}H_9O_4]^-$ Ferulate, *m/z* 175=$[C_{10}H_7O_3]^-$, see also Santos and Graça, *Holzforschung* (2006) **60**, 171-177

Supplemental Table 7. Analytical Data of Alkyl Ferulates Detected by UPLC/ESI(-)-QTOFMS.

analyte	elemental comp.	ret. time [s]	quantifier ion				prominent fragment ions upon CID
			type	measured *m/z*	error *ppm*	mSigma[1]	precursor ion@collision energy: *m/z* (rel. int. [%], ion type[3])
C16:0	$C_{26}H_{42}O_4$	612[2]	$[M-H]^-$	417.2988	5.3	6.5	**417@30 eV:** 417 (2), 402 (100, **a**), 177 (8), 133 (10)
C18:0	$C_{28}H_{46}O_4$	695[2]	$[M-H]^-$	445.3306	3.9	4.8	**445@30 eV:** 445 (7), 430 (100, **a**), 177 (5), 133 (6)
C19:0	$C_{29}H_{48}O_4$	732[2]	$[M-H]^-$	459.3462	3.9	4.1	**459@30 eV:** 459 (10), 444 (100, **a**), 177 (4), 133 (6)
C20:0	$C_{30}H_{50}O_4$	767[2]	$[M-H]^-$	473.3618	3.9	4.4	**473@30 eV:** 473 (16), 458 (100, **a**), 177 (3), 133 (3)
C21:0	$C_{31}H_{52}O_4$	800[2]	$[M-H]^-$	487.3773	4.1	1.3	**487@30 eV:** 487 (21), 472 (100, **a**), 177 (3), 133 (2)
C22:0	$C_{32}H_{54}O_4$	832[2]	$[M-H]^-$	501.3925	4.8	1.0	**501@30 eV:** 501 (31), 486 (100, **a**), 177 (2), 133 (2)
C23:0	$C_{33}H_{56}O_4$	859[2]	$[M-H]^-$	515.4094	2.3	9.7	**515@40 eV:** 515 (4), 500 (100, **a**), 177 (13), 133 (43)
C24:0	$C_{34}H_{58}O_4$	886[2]	$[M-H]^-$	529.4250	2.3	3.9	**529@40 eV:** 529 (1), 514 (100, **a**), 177 (18), 133 (34)
C25:0	$C_{35}H_{60}O_4$	910[2]	$[M-H]^-$	543.4404	2.7	14	**543@40 eV:** 543 (1), 528 (100, **a**), 177 (17), 133 (20)
C26:0	$C_{36}H_{62}O_4$	930[2]	$[M-H]^-$	557.4558	3.1	11	**557@40 eV:** 557 (5), 542 (100, **a**), 177 (10), 133 (22)
C27:0	$C_{37}H_{64}O_4$	952[2]	$[M-H]^-$	571.4722	1.7	29	**571@40 eV:** 571 (11), 556 (100, **a**), 177 (10), 133 (6)
C28:0	$C_{38}H_{66}O_4$	973[2]	$[M-H]^-$	585.4867	3.6	4.1	**585@40 eV:** 585 (10), 570 (100, **a**), 177 (6), 133 (12)

[1] goodness of fit between measured and calculated isotope pattern (Bruker Daltonics, Data Analysis 4.0)
[2] major (*E*)-isomer, minor (*Z*)-isomer elutes 20 s later, isomer ratio (E)/(Z) in the range from 8:1 to 12:1
[3] elemental composition of fragment ions supported by accurate mass measurements (± 15 ppm), **a**=$[M-H-CH_3]^{\bullet-}$, *m/z* 177=$[C_9H_5O_4]^-$, *m/z* 133=$[C_8H_5O_2]^-$

Supplemental Table 8. Analytical Data of Hydroxyalkyl Ferulates Detected by UPLC/ESI(-)-QTOFMS.

analyte	elemental comp.	ret. time [s]	quantifier ion				prominent fragment ions upon CID
			type	measured *m/z*	error *ppm*	mSigma[a]	precursor ion@collision energy: *m/z* (rel. int. [%], ion type[3])
C18:0	$C_{28}H_{46}O_5$	441[b]	$[M-H]^-$	461.3262	2.3	18	**461@40 eV:** 461 (1), 446 (60, **a**), 177 (31), 133 (100)
C20:0	$C_{30}H_{50}O_5$	535[b]	$[M-H]^-$	489.3569	3.4	9.3	**489@40 eV:** 489 (1), 474 (82, **a**), 177 (31), 133 (100)
C21:0	$C_{31}H_{52}O_5$	577[b]	$[M-H]^-$	503.3734	1.6	4.3	**503@40 eV:** 503 (1), 488 (100, **a**), 177 (28), 133 (72)
C22:0	$C_{32}H_{54}O_5$	620[b]	$[M-H]^-$	517.3892	1.3	1.9	**517@40 eV:** 517 (1), 502 (100, **a**), 177 (21), 133 (48)
C24:0	$C_{34}H_{58}O_5$	699[b]	$[M-H]^-$	545.4175	6.7	21	**545@40 eV:** 545 (8), 530 (100, **a**), 177 (14), 133 (30)

[1] goodness of fit between measured and calculated isotope pattern (Bruker Daltonics, Data Analysis 4.0)
[2] major (*E*)-isomer, minor (*Z*)-isomer elutes 20 s later, isomer ratio (E)/(Z) in the range from 10:1 to 20:1
[3] elemental composition of fragment ions supported by accurate mass measurements (± 15 ppm), **a**=$[M-H-CH_3]^{\bullet-}$, *m/z* 177=$[C_9H_5O_4]^-$, *m/z* 133=$[C_8H_5O_2]^-$

Supplemental Table 9. Analytical Data of Feruloyloxyalkyl Ferulates Detected by UPLC/ESI(-)-QTOFMS.

analyte	elemental comp.	ret. time [s]	quantifier ion				prominent fragment ions upon CID
			type	measured *m/z*	error *ppm*	mSigma[a]	precursor ion@collision energy: *m/z* (rel. int. [%], ion type[3])
C16:0	$C_{36}H_{50}O_8$	507[b]	$[M-H]^-$	609.3446	2.1	9.3	**609@30 eV:** 609 (28), 594 (6, **a**), 433 (100, **b**), 418 (21, **c**), 401 (12, **d**), 193 (9), 175 (50)
C18:0	$C_{38}H_{54}O_8$	587[b]	$[M-H]^-$	637.3746	0.0	6.2	**637@30 eV:** 637 (37), 622 (7, **a**), 461 (100, **b**), 446 (14, **c**), 429 (10, **d**), 193 (9), 175 (55)
C20:0	$C_{40}H_{58}O_8$	660[b]	$[M-H]^-$	665.4037	3.3	30	**665@30 eV:** 665 (50), 650 (6, **a**), 489 (100, **b**), 474 (9, **c**), 457 (9, **d**), 193 (9), 175 (72)
C22:0	$C_{42}H_{62}O_8$	727[b]	$[M-H]^-$	693.4365	1.0	12	**693@30 eV:** 693 (71), 678 (5, **a**), 517 (100, **b**), 502 (7, **c**), 485 (8, **d**), 193 (11), 175 (75)
C24:0	$C_{44}H_{66}O_8$	786[b]	$[M-H]^-$	721.4671	1.9	12	**721@30 eV:** 721 (100), 706 (3, **a**), 545 (84, **b**), 530 (3, **c**), 513 (3, **d**), 193 (10), 175 (74)

[a] goodness of fit between measured and calculated isotope pattern (Bruker Daltonics, Data Analysis 4.0)
[b] major (*E*),(*E*)-isomer, minor (*E*),(*Z*)-isomer elutes 18 s later, isomer ratio (*E*),(*E*)/(*E*),(*Z*) in the range from 10:1 to 20:1
[c] elemental composition of fragment ions supported by accurate mass measurements (± 15 ppm), **a**=$[M-H-CH_3]^{\bullet-}$, **b**=$[M-H-C_{10}H_8O_3]^-$, **c**=$[M-H-C_{10}H_8O_3-CH_3]^{\bullet-}$, **d**=$[M-H-C_{10}H_8O_3-CH_4O]^-$, *m/z* 193=$[C_{10}H_9O_4]^-$ Ferulate, *m/z* 175=$[C_{10}H_7O_3]^-$

Supplemental Table 10. Relative quantification of ferulic acid conjugates, ω-hydroxy fatty acids, α,ω-dicarboxylic acids and fatty acids in apolar extracts of *ABCG1*-RNAi and control periderm.

Methyl *tert*-butyl ether extracts of *ABCG1*-RNAi [four independent lines (n=32)] and control [wild type (n=8), empty vector (n=8)] tuber periderm were prepared and analyzed by UPLC/PDA/ESI(-)-QTOFMS. Target compounds were relatively quantified using quantifier ions/retention times from Supplemental Material 1. Resulting peak areas were normalized to fresh weight and $\log_2$-transformed. Shown values represent medians ± **SD**. Significance analysis of differences between *ABCG1*-RNAi and control was performed by *t*-test (two-tailed, unequal variances): $^{*}P \leq 0.05$; $^{**}P \leq 0.01$; $^{***}P \leq 0.001$. "-" indicates that the corresponding quantifier ion was below the detection limit.

Chain Length	Compound Class / Median Response ± sd							
	Feruloyloxy Fatty Acids		Feruloyloxy Fatty Acid Glycerol Esters		Alkyl Ferulates		Hydroxyalkyl Ferulates	
	control	*RNAi*	*control*	*RNAi*	*control*	*RNAi*	*control*	*RNAi*
C16:0	6.6 ± 0.4	10.8 ± 1.3***	6.9±0.4	11.0 ± 0.6***	13.2±1.1	10.9 ± 2.0***	-	-
C16:1	-	-	-	-	-	-	-	-
C17:0	-	-	-	-	-	-	-	-
C18:0	5.7±0.9	11.0± 1.1***	-	12.7 ± 0.8	11.3 ± 0.2	12.5 ± 0.7***	-	9.7 ± 1.0
C18:1	6.7±1.1	12.6±1.6***	7.6±0.9	12.3±0.7***	-	-	-	-
C18:2	5.6±0.5	9.0±0.7***	-	11.0±0.5	-	-	-	-
C18:3	-	-	-	-	-	-	-	-
C19:0	-	8.7±0.8	-	8.8±0.9	9.9±0.2	11.0±1.3***	-	-
C20:0	6.8±0.3	14.9±0.7***	8.0±0.5	16.3±0.5***	9.9±0.3	12.8±0.4***	-	10.9±0.7
C21:0	7.0±0.4	11.2±0.7***	-	13.1±0.6	12.1±0.2	11.3±1.2***	12.1±0.2	10.9±0.9***
C22:0	10.5±0.3	15.8±0.5***	13.1±0.4	17.5±0.3***	11.4±0.1	12.8±0.7***	10.2±0.3	13.7±0.3***
C23:0	8.5±0.3	10.4±0.4***	9.1±0.3	14.4±0.5***	11.2±0.2	9.3±0.6***	-	-
C24:0	10.7±0.4	14.2±0.7***	12.9±0.4	16.3±0.3***	11.6±0.2	11.8±0.8	7.8±0.6	10.5±0.4***
C25:0	5.4±0.7	8.7±0.2***	7.8±0.3	11.7±0.4***	10.3±0.1	9.7±0.8***	-	-
C26:0	8.6±0.3	11.8±0.4***	11.9±0.3	13.8±0.6***	11.0±0.1	11.2±1.4	-	-
C27:0	-	-	-	-	8.4±0.3	8.6±1.4	-	-
C28:0	8.7±0.2	10.5±0.7***	9.1±0.7	10.2±2.1	11.0±0.7	10.6±2.0**	-	-
C29:0	-	-	-	-	-	-	-	-
C30:0	-	-	-	-	-	-	-	-

Chain Length	Compound Class / Median Response ± sd							
	Feruloyloxyalkyl Ferulates		ω-Hydroxy Fatty Acids		α,ω-Dicarboxylic Acids		Fatty Acids	
	control	*RNAi*	*control*	*RNAi*	*control*	*RNAi*	*control*	*RNAi*
C16:0	11.6± 0.5	12.3 ± 2.4	-	-	-	-	11.4± 0.3	12.6 ± 0.7***
C16:1	-	-	-	-	-	-	4.9±1.2	9.2±1.0***
C17:0	-	-	-	-	-	-	5.7±1.0	9.9±1.0***
C18:0	8.4 ± 0.2	12.3 ± 0.8***	-	-	-	-	11.4 ± 0.2	13.4± 0.5***
C18:1	-	-	-	-	-	-	9.3±0.5	14.0±1.0***
C18:2	-	-	-	-	-	-	12.7±0.3	12.8±0.5
C18:3	-	-	-	-	-	-	10.1±0.2	10.5±0.6***
C19:0	-	-	-	-	-	-	4.8±0.5	8.8±0.7***
C20:0	8.0±0.9	12.1±0.3***	-	11.3±1.1	-	10.7±1.5	8.0±0.3	11.9±0.4***
C21:0	-	-	-	8.2±1.0	-	7.6±1.1	5.8±0.5	9.5±0.5***
C22:0	10.7±0.3	12.9±0.1***	7.2±0.3	13.0±0.7***	5.2±0.4	11.7±1.3***	9.4±0.5	11.3±0.3***
C23:0	-	-	-	9.0±0.8	-	7.9±1.0	6.8±0.5	10.01±0.2***
C24:0	7.7±0.6	10.6±0.4***	8.7±0.2	12.3±0.5***	6.6±0.3	11.5±0.8***	11.1±0.2	12.1±0.1***
C25:0	-	-	-	-	-	-	8.9±0.3	11.1±0.2***
C26:0	-	-	9.1±0.2	10.7±0.5***	6.8±0.3	9.2±0.6***	12.5±0.1	12.9±0.5
C27:0	-	-	-	-	-	-	9.9±0.2	10.7±1.2
C28:0	-	-	8.9±0.5	9.1±0.8	7.6±0.3	8.0±0.9*	13.9±0.1	13.5±1.4**
C29:0	-	-	-	-	-	-	12.8±0.1	10.7±1.3***
C30:0	-	-	-	-	-	-	11.7±0.1	10.1±0.7***

Supplemental Table 11. Analytical Data of Aromatic Amino Acids, Phenylpropanoids, Anthocyanins and Glycoalkaloids Detected by UPLC/ESI(+)-QTOFMS.

compound	elemental comp.	ret. time [s]	quantifier ion				observed fragment ions upon CID
			type	measured *m/z*	error *ppm*	mSigma[1]	precursor ion@collision energy: *m/z* (rel. int. [%], elemental composition)
Phe[3]	$C_9H_{11}NO_2$	135	$[M+H]^+$	166.0859	2.1	1.8	**166@10eV:** 166 (8, $C_9H_{12}NO_2^+$), 149 (3, $C_9H_9O_2^+$), 131 (5, $C_9H_7O^+$), 120 (100, $C_8H_{10}N^+$), 107 (1, $C_7H_7O^+$), 103 (3, $C_8H_7^+$)
Tyr[3]	$C_9H_{11}NO_3$	79	$[M+H]^+$	182.0804	4.1	5.1	**182@10eV:** 182 (9, $C_9H_{12}NO_3^+$), 165 (66, $C_9H_9O_3^+$), 147 (19, $C_9H_7O_2^+$), 136 (100, $C_8H_{10}NO^+$), 123 (26, $C_7H_7O_2^+$), 119 (12, $C_8H_7O^+$), 91 (2, $C_7H_7^+$)
Trp[3]	$C_{11}H_{12}N_2O_2$	175	$[M+H]^+$	205.0970	0.9	2.2	**205@10eV: 205** (2, $C_{11}H_{13}N_2O_2^+$), 188 (100, $C_{11}H_{10}NO_2^+$), 159 (4, $C_{10}H_{11}N_2^+$), 132 (2, $C_9H_{10}N^+$)
Caffeic acid[3]	$C_9H_8O_4$	219	$[M+H]^+$	181.0496	0.4	5.6	**181@15eV:** 163 (100, $C_9H_7O_3^+$), 145 (55, $C_9H_5O_2^+$), 135 (50, $C_8H_7O_2^+$), 117 (19, $C_8H_5O^+$),
Chlorogenic Acid[3]	$C_{16}H_{18}O_9$	204/210	$[M+H]^+$	355.1010	3.9	6.9	**355@15eV:** 337 (1, $C_{16}H_{17}O_8^+$), 181 (1, $C_9H_9O_4^+$), 163 (100, $C_9H_7O_3^+$), 145 (2, $C_9H_5O_2^+$)
Cinnamoyl putrescine	$C_{13}H_{18}N_2O$	242	$[M+H]^+$	219.1480	5.4	11.0	**219@10eV:** 219 (81, $C_{13}H_{19}N_2O^+$), 202 (100, $C_{13}H_{16}NO^+$), 131 (42, $C_9H_7O^+$)
Coumaroyl putrescine	$C_{13}H_{18}N_2O_2$	182	$[M+H]^+$	235.1428	5.6	3.2	**235@10eV:** 235 (100, $C_{13}H_{19}N_2O_2^+$), 218 (100, $C_{13}H_{16}NO_2^+$), 147 (97, $C_9H_7O_2^+$)
Caffeoyl putrescine[4]	$C_{13}H_{18}N_2O_3$	163	$[M+H]^+$	251.1397	2.6	2.5	**251@15eV:** 251 (4, $C_{13}H_{19}N_2O_3^+$), 234 (13, $C_{13}H_{16}NO_3^+$), 163 (100, $C_9H_7O_3^+$), 145 (4, $C_9H_5O_2^+$), 135 (2, $C_8H_7O_2^+$)
Dihydrocaffeoyl putrescine	$C_{13}H_{20}N_2O_3$	138	$[M+H]^+$	253.1542	1.7	2.8	**253@15eV:** 253 (20, $C_{13}H_{21}N_2O_3^+$), 236 (100, $C_{13}H_{18}NO_3^+$), 165 (20, $C_9H_9O_3^+$), 123 (7, $C_7H_7O_2^+$)
Feruloyl putrescine[4]	$C_{14}H_{20}N_2O_3$	197	$[M+H]^+$	265.1546	0.4	1.5	**265@15eV:** 265 (3, $C_{14}H_{21}N_2O_3^+$), 248 (5, $C_{14}H_{18}NO_3^+$), 177 (100, $C_{10}H_9O_3^+$), 149 (1, $C_9H_9O_2^+$), 145 (9, $C_9H_5O_2^+$)
Dihydroferuloyl putrescine	$C_{14}H_{22}N_2O_3$	174	$[M+H]^+$	267.1695	3.2	1.8	**267@15eV:** 267 (29, $C_{14}H_{23}N_2O_3^+$), 250 (100, $C_{14}H_{20}NO_3^+$), 179 (15, $C_{10}H_{11}O_3^+$), 137 (15, $C_8H_9O_2^+$)
Vanilloyl putrescin	$C_{12}H_{18}N_2O_3$	153	$[M+H]^+$	239.1390	0.2	5.0	**239@15eV:** 239 (5, $C_{12}H_{19}N_2O_3^+$), 222(30, $C_{12}H_{16}NO_3^+$), 151(100, $C_8H_7O_3^+$) **239@30eV:** 151(100, $C_8H_7O_3^+$), 141(11, $C_7H_9O_3^+$), 123(36, $C_7H_7O_2^+$), 108(9, $C_6H_4O_2^{+\bullet}$)
Feruloyl tyramine (FT)[4]	$C_{18}H_{19}NO_4$	353	$[M+H]^+$	314.1383	1.3	2.5	**314@15eV:** 314 (24, $C_{18}H_{20}NO_4^+$), 194 (2, $C_{10}H_{12}NO_3^+$), 177 (100, $C_{10}H_9O_3^+$), 145 (5, $C_{19}H_5O_2^+$), 121 (6, $C_8H_9O^+$)
Feruloyl octopamine (FO)[4]	$C_{18}H_{19}NO_5$	290	$[M+H-H_2O]^+$	312.1212	5.8	6.7	**330@15eV:** 312 (6, $C_{18}H_{18}NO_4^+$), 177 (100, $C_{10}H_9O_3^+$), 145 (5, $C_{10}H_5O_2^+$)
FT-FT Dehydrodimer[4]	$C_{36}H_{36}N_2O_8$	458	$[M+H]^+$	625.2531	2.2	5.7	**625@15eV:** 625 (99, $C_{36}H_{37}N_2O_8^+$), 488 (21, $C_{28}H_{26}NO_7^+$), 462 (100, $C_{27}H_{28}NO_6^+$), 351 (17, $C_{20}H_{15}O_6^+$), 325 (45, $C_{19}H_{17}O_5^+$), 299 (2, $C_{18}H_{19}O_4^+$)
FT-FO Dehydrodimer[4]	$C_{36}H_{36}N_2O_9$	407	$[M+H]^+$	641.2598	0.7	-[2]	**641@15eV:** 623 (28, $C_{36}H_{35}N_2O_9^+$), 517 (3, $C_{29}H_{29}N_2O_7^+$), 488 (26, $C_{28}H_{26}NO_7^+$), 486 (33, $C_{28}H_{24}NO_7^+$), 462 (100, $C_{27}H_{28}NO_6^+$), 460 (33, $C_{27}H_{26}NO_6^+$), 380 (5, $C_{21}H_{18}NO_6^+$), 351 (58, $C_{20}H_{15}O_6^+$), 325 (97, $C_{19}H_{17}O_5^+$)
Pelargonidin-3-(coumaroyl-Rha-Glc)-5-Glc[5,6]	$C_{42}H_{47}O_{21}^+$	272	$[M]^+$	887.2567	4.2	9.0	**887@40eV:** 887 (1), 725 (12, $C_{36}H_{37}O_{16}^+$), 433 (61, $C_{21}H_{21}O_{10}^+$), 271 (100, $C_{15}H_{11}O_5^+$)
Pelargonidin-3-(feruloyl-Rha-Glc)-5-Glc[5,6]	$C_{43}H_{49}O_{22}^+$	277	$[M]^+$	917.2659	5.5	7.5	**917@40eV:** 917 (1), 755 (10, $C_{37}H_{39}O_{17}^+$), 433 (70, $C_{21}H_{21}O_{10}^+$), 271 (100, $C_{15}H_{11}O_5^+$)
α-Solanine	$C_{45}H_{73}NO_{15}$	358	$[M+H]^+$	868.5041	1.4	4.7	**in-source CID:** 868 (73), 850 (1, $C_{45}H_{72}NO_{14}^+$), 722 (5, $C_{39}H_{64}NO_{11}^+$), 706 (1, $C_{39}H_{64}NO_{10}^+$), 560 (47, $C_{33}H_{54}NO_6^+$), 446 (100, $C_{45}H_{74}NO_{15}Na^{2+}$), 398 (67, $C_{27}H_{44}NO^+$), 309 (29, $C_{12}H_{21}O_9^+$)
α-Chaconine	$C_{45}H_{73}NO_{14}$	361	$[M+H]^+$	852.5112	1.0	6.1	**in-source CID:** 852 (100), 706 (67, $C_{39}H_{64}NO_{10}^+$), 560 (41, $C_{33}H_{54}NO_6^+$), 438 (29, $C_{45}H_{74}NO_{14}Na^{2+}$), 398 (11, $C_{27}H_{44}NO^+$)

[1] goodness of fit between measured and calculated isotope pattern (Bruker Daltonics, Data Analysis 4.0)
[2] isotope pattern interfered by co-eluting compound
[3] identified using a commercially available reference compound
[4] Serra et al., *Plant J.* (2010) **62**, 277-290, see Supplemental Methods 1 and literature cited therein
[5] Sachse, *Z. Lebensm. Unters. Forsch.* (1973) **153**, 294-300
[6] Lewis et al., *J. Sci. Food Agric.* (1998) **77**, 45-57

Supplemental Table 12. Analytical Data of ω-Hydroxy Fatty Acids Detected by UPLC/ESI(-)-QTOFMS.

analyte	elemental comp.	ret. time [s]	quantifier ion			
			type	measured *m/z*	error *ppm*	mSigma[1]
C20:0	$C_{20}H_{40}O_3$	326	$[M-H]^{-2}$	327.2902	0.8	6.0
C21:0	$C_{21}H_{42}O_3$	379	$[M-H]^{-2}$	341.3075	4.0	8.7
C22:0	$C_{22}H_{44}O_3$	430	$[M-H]^{-2}$	355.3214	1.0	4.1
C23:0	$C_{23}H_{46}O_3$	481	$[M-H]^{-2}$	369.3372	0.6	2.7
C24:0	$C_{24}H_{48}O_3$	529	$[M-H]^{-2}$	383.3524	1.7	2.5
C26:0	$C_{26}H_{52}O_3$	622	$[M-H]^{-2}$	411.3837	1.6	8.5
C28:0	$C_{28}H_{56}O_3$	707	$[M-H]^{-2}$	439.4131	5.8	6.1

[1] goodness of fit between measured and calculated isotope pattern (Bruker Daltonics, Data Analysis 4.0)
[2] The CID mass spectrum obtained from $[M-H]^-$ at 20 eV shows the fragment ions $[M-H-H_2O]^-$, $[M-H-HCOOH]^-$.
The commercially available standards 15-hydroxypentadecanoic acid and 16-hydroxydecanoic acid show similar CID mass spectra.

Supplemental Table 13. Analytical Data of α,ω-Dicarboxylic Acids Detected by UPLC/ESI(-)-QTOFMS.

analyte	elemental comp.	ret. time [s]	quantifier ion			
			type	measured *m/z*	error *ppm*	mSigma[1]
C20:0	$C_{20}H_{38}O_4$	297	$[M-H]^{-2}$	341.2694	1.0	4.1
C21:0	$C_{21}H_{40}O_4$	347	$[M-H]^{-2}$	355.2842	3.3	15
C22:0	$C_{22}H_{42}O_4$	398	$[M-H]^{-2}$	369.3011	0.2	4.2
C23:0	$C_{23}H_{44}O_4$	447	$[M-H]^{-2}$	383.3156	2.8	31
C24:0	$C_{24}H_{46}O_4$	494	$[M-H]^{-2}$	397.3308	3.9	10
C26:0	$C_{26}H_{50}O_4$	584	$[M-H]^{-2}$	425.3634	0.5	30
C28:0	$C_{28}H_{54}O_4$	668	$[M-H]^{-2}$	453.3924	5.6	32

[1] goodness of fit between measured and calculated isotope pattern (Bruker Daltonics, Data Analysis 4.0)
[2] The CID mass spectrum obtained from $[M-H]^-$ at 20 eV shows the fragment ions $[M-H-H_2O]^-$, $[M-H-CO_2]^-$, $[M-H-H_2O-CO_2]^-$.
The commercially available standards hexadecanedioic acid and octadecanediocic acid show similar CID mass spectra.

Supplemental Table 14. Analytical Data of Fatty Acids Detected by UPLC/ESI(-)-QTOFMS.

analyte	elemental comp.	ret. time [s]	quantifier ion			
			type	measured *m/z*	error *ppm*	mSigma[1]
C16:0[3]	$C_{16}H_{32}O_2$	407	$[M-H]^{-2}$	255.2332	1.0	4.2
C16:1	$C_{16}H_{30}O_2$	340	$[M-H]^{-2}$	253.2171	0.8	4.9
C17:0[3]	$C_{17}H_{34}O_2$	461	$[M-H]^{-2}$	269.2486	0.0	4.4
C18:0[3]	$C_{18}H_{36}O_2$	513	$[M-H]^{-2}$	283.2641	0.5	6.1
C18:1	$C_{18}H_{34}O_2$	439	$[M-H]^{-2}$	281.2483	1.1	5.6
C18:2	$C_{18}H_{32}O_2$	371	$[M-H]^{-2}$	279.2333	1.3	2.0
C18:3	$C_{18}H_{30}O_2$	312	$[M-H]^{-2}$	277.2170	1.1	10
C19:0[3]	$C_{19}H_{38}O_2$	563	$[M-H]^{-2}$	297.2789	3.4	7.7
C20:0[3]	$C_{20}H_{40}O_2$	610	$[M-H]^{-2}$	311.2946	3.1	9.9
C21:0[3]	$C_{21}H_{42}O_2$	657	$[M-H]^{-2}$	325.3108	1.2	7.9
C22:0[3]	$C_{22}H_{44}O_2$	700	$[M-H]^{-2}$	339.3263	1.6	2.0
C23:0[3]	$C_{23}H_{46}O_2$	739	$[M-H]^{-2}$	353.3411	4.0	2.4
C24:0[3]	$C_{24}H_{48}O_2$	778	$[M-H]^{-2}$	367.3569	3.4	3.0
C25:0[3]	$C_{25}H_{50}O_2$	813	$[M-H]^{-2}$	381.3721	4.5	8.0
C26:0[3]	$C_{26}H_{52}O_2$	846	$[M-H]^{-2}$	395.3887	1.9	4.3
C27:0[3]	$C_{27}H_{54}O_2$	875	$[M-H]^{-2}$	409.4039	3.0	10
C28:0[3]	$C_{28}H_{56}O_2$	901	$[M-H]^{-2}$	423.4191	3.9	6.6
C29:0[3]	$C_{29}H_{58}O_2$	925	$[M-H]^{-2}$	437.4349	3.5	13
C30:0[3]	$C_{30}H_{60}O_2$	950	$[M-H]^{-2}$	451.4501	4.3	34

[1] goodness of fit between measured and calculated isotope pattern (Bruker Daltonics, Data Analysis 4.0)
[2] In accordance with the literature (Schiesel et al., *Anal. Bioanal. Chem.* (2010) **397**, 147-160), the CID mass spectra obtained from $[M-H]^-$ in a collision energy range of 10-40 eV do not show prominent fragment ions.
[3] identified using a commercially available reference compound

Supplemental Table 15. Analytical Data of Trimethylsilyloxycinnamic Acid Methyl Esters Detected by GC/EI-QMS.

analyte	elemental comp.	M	ret. time *[min]*	quantifier ion *m/z* (rel. int.[%])	qualifier ions *m/z* (rel. int.[%])		MF[1]	internal standard for quantification
Methyl coumarate (1TMS)[2]	$C_{13}H_{18}O_3Si$	250	9.11	250 (100)	235 (70)	219 (40)	642	methyl heptadecanoate
Methyl coumarate (1TMS)[3]	$C_{13}H_{18}O_3Si$	250	10.13	250 (100)	235 (70)	219 (40)	869	methyl heptadecanoate
Methyl ferulate (1TMS)[2]	$C_{14}H_{20}O_4Si$	280	10.54	250 (100)	280 (40)	265 (16)	870	methyl heptadecanoate
Methyl ferulate (1TMS)[3]	$C_{14}H_{20}O_4Si$	280	11.92	250 (100)	280 (40)	265 (16)	882	methyl heptadecanoate

[1] match factor obtained from NIST MS Search 2.0 using NIST/EPA/NIH Mass Spectral Library 2011
[2] minor isomer
[3] major isomer